An Instantaneous Event-Triggered Hz-Watt Control for Microgrids

Babak Abdolmaleki, *Member, IEEE,* Qobad Shafiee, *Senior Member, IEEE,*
Mohammad Mehdi Arefi, *Senior Member, IEEE,* and Tomislav Dragičević, *Senior Member, IEEE*

***Abstract*—This paper proposes a distributed control scheme to compensate for droop-induced frequency deviations in autonomous microgrids. In this scheme, no extra direct frequency control and proportional-integral compensation are employed to remove the frequency deviations; that is, the deviations are compensated instantaneously. To reduce the communication burden, the scheme is then equipped with a need-based (event-triggered) data exchange strategy. An event-triggering mechanism is introduced which, *i*) highly reduces the amount of communications in both transient and steady-state stages and *ii*) ensures that the intervals between consecutive communication instants are positive (i.e., the system is Zeno-free). Stability and equilibrium analyses of the resultant system considering the whole system dynamics are provided, as well. Effectiveness of the proposed controller for different cases is verified by simulating a microgrid in MATLAB/SimPowerSystems software environment.**

***Index Terms*—Droop control, event-triggered control, frequency control, microgrid, secondary control, Zeno behavior.**

I. Introduction

DROOP-CONTROL provides a solution to penetrate multiple inverter-interfaced distributed generations (DGs) into the microgrids (MGs), simultaneously. Despite its simple, cheap, and reliable functionality, this controller deviates the DGs' voltages and frequencies from the nominal values [1], [2]. These deviations can be compensated by shifting the droop characteristics along the voltage and frequency axes, via including correction terms in the droop equations [2], [3].

In the MG control hierarchy, secondary control is responsible to determine the correction terms in a centralized or decentralized or distributed fashion [2], [4]. In the centralized methods, the DGs information are all gathered in a central unit, where proper correction terms are computed and sent back to the DGs. These methods, however, require a complex communication network between the central control unit and the DGs; hence, they are not scalable and reliable (since the central unit exhibits a single point of failure) [4]. On the other hand, decentralized and distributed methods are more reliable and scalable; the former needs no communication, while the latter requires sparse inter-DG data exchange network. The decentralized methods may utilize change detection techniques [5] or distributed low-pass filters [6]. The former does not react to the load variations instantaneously [5] and the latter acts properly only for high-load conditions [6]. The third group contains the distributed secondary controllers that utilize DG-to-DG data exchange network and that generate the secondary frequency correction terms locally. In this group however, because of their scalability and lower costs, the cosensus-based schemes using neighbor-to-neighbor communications [7]–[20] are preffered to the other methods with all-to-all communications [21], [22]. In [7], a secondary controller based on the average and leader-following consensus algorithms is proposed. In order to improve the performance of this controller, some finite-time [8]–[10] and adaptive [11] control techniques have been utilized in the literature. A distributed cooperative secondary controller, using cost-based droop control, is proposed in [12]. Reference [13] investigates the optimal operation of the proposed controller in [12] but with conventional droop control scheme. In [14], a consensus and containment-based control is proposed which tries to share the DGs' reactive powers proerly while keeping voltages within an allowable range. In [15], [16], some consensus-based secondary voltage and frequency controllers are proposed. The eqilibrium and stability analyses of the frequency and active power sharing (Hz-Watt) problem in [16] are invenstigated in [17], [18] while the voltage and reactive power sharing (Volt-VAr) problem is studied in [19]. A droop-free consensus-based Volt-VAr controller is proposed in [20] under which, the conventional voltage droop controller is replaced by a first order controller.

Most of the existing secondary controllers are conducted based on continuous communications, e.g., the above mentioned works. However, the real communication channels are not continuous and have limited bandwidths [23]. Hence, considering the MG as a networked control system, the communication network among the DGs is a limited and shared resource; therefore, saving the communications seems to be mandatory [24]. A solution for efficient usage of digital communication infrastructures is to use event-triggered control strategies [25]–[27]. In these strategies, broadly speaking, an event is detected (i.e., the desired signal is sampled and transmitted), only if some measurement error violates a predefined threshold. Any event-triggering condition must meet two system's requirements; *i*) stability, and *ii*) Zeno-freeness

Manuscript received MM DD, 2018; revised MM DD, 2018; accepted MM DD, 2019. Date of publication MM DD, 2019; date of current version MM DD, 2019.

B. Abdolmaleki and Q. Shafiee are with the Smart/Micro Grids Research Center (SMGRC), University of Kurdistan, Sanandaj 66177-15175, Iran (e-mails: abdolmaleki.p.e@gmail.com; q.shafiee@uok.ac.ir).

M. M. Arefi is with the School of Electrical and Computer Engineering, Shiraz University, Shiraz 71348-51154, Iran (e-mail: arefi@shirazu.ac.ir).

T. Dragičević is with the Department of Energy Technology, Aalborg University, 9220 Aalborg, Denmark (e-mail: tdr@et.aau.dk).

Color versions of one or more of the figures in this paper are available online at http://ieeexplore.ieee.org.

Digital Object Identifier XXX

[26]. Zeno behavior is a phenomenon under which, excessive triggers (sampling or communication) occur over a finite time interval. Due to the limited communication and computational capabilities, no control system can be implemented on a digital platform in the presence of this behavior [26]. Therefore, the system should be Zeno-free [25]–[27].

Event-triggered control has been already investigated in the power systems literature [28]–[33]. Event-triggered load frequency control of multi-area power systems is proposed in [28]. The proposed event-triggering mechanism guarantees the stability of the closed-loop system. In [29], a distributed load sharing strategy with event-triggered communications is proposed. In this work, only the active power sharing of inverters is investigated and the DGs' volatges and frequencies are not controlled. In [30], a distributed event-triggered reactive power sharing strategy is presented. In this work, a new consensus-based control with nonlinear state feedbacks is introduced which provides accurate reactive power sharing among the DGs; however, the Hz-Watt problem is not investigated. An event-triggered voltage, frequency, and load sharing control is presented in [31]. The utilized event-triggering conditions have no constant threshold; therefore, over the steady-state stage when the synchronization is achieved, Zeno behavior may happen (see Section III of [26] for more details). In [32], a distributed event-triggered secondary Hz-Watt control for MGs is proposed. The utilized event-triggered is intrinsically Zeno-free; however, the number of communications in steady-state is not reduced significantly. Besides, the controllers in [31], [32], similar to the ones in [7]–[11], are based on the feedback linearization technique and defining auxiliary control inputs. Therefore, the whole MG dynamics including DGs and electrical network model are not considered. In [33], an event-triggered voltage, frequency and power sharing control strategy is provided. The controller design is based on the $P-f/Q-\dot{V}$ droop mechanisms proposed in [15].

The secondary correction term is conventionally generated by proportional-integral (PI) action. For example, all the above event-triggered and non-event-triggered methods utilize a PI controller in a centralized or decentralized or distributed manner. However, the control loops after the droop control, have an integrator per se, converting the frequency to phase angle. Thus, it seems to be simpler and more instantaneous to use this property for Hz-Watt control, without the use of a PI controller in the secondary level. This motivates the study in this paper to introduce an instantaneous Hz-Watt control scheme, which benefits from need-based communications between the DGs.

Motivated by the above statements and inspired by the consensus algorithm in [34], a distributed frequency restoration control for islanded inverter-based MGs is proposed in this paper. Prominent advantages of the method over the conventional ones are as follows.

- The average of droop-induced frequency deviations, associated with each DG's neighbors, is utilized as compensation term. Hence, no extra PI controller is required to generate compensation terms; indeed they are produced *instantaneously* by using algebraic operations on the latest received data from neighboring DGs.

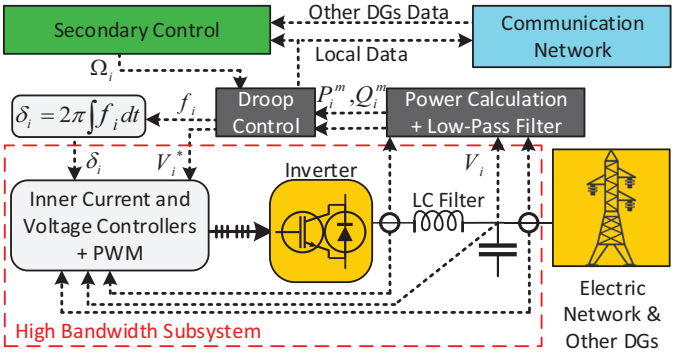

Fig. 1. Overall model of i^{th} DG in a hierarchically droop-controlled microgrid.

- An event-triggering mechanism is introduced, which employs a triggering condition with both state-dependent and constant parts. The mechanism reduces the communication burden in both transient and steady-state stages and ensures that the system is stable and Zeno-free.

The rest of this paper is organized as follows. Section II provides the system modeling. The conventional and the proposed Hz-Watt control scheme as well as the event-triggered data exchange strategy are introduced in Section III, where the design points are given as well. The effectiveness of the proposed method, for different case studies, has been validated by simulating an inverter-based MG in MATLAB/SimPowerSystems software environment, and the results are included in Section IV. Finally, Section V concludes the paper.

II. System Modeling

A hierarchically controlled MG consists of three parts including communication network, hierarchically controlled DGs, and electrical network. Fig. 1 depicts an overview of the MG system. Next, each part is mathematically modeled.

A. Communication Layer (Graph Theory)

The communication network among DGs, can be regarded as a graph with DGs and communication links playing the roles of its nodes and edges, respectively. Consider the graph $\mathcal{G}=(\mathcal{N},\mathcal{E},\mathcal{A})$, where, $\mathcal{N}=\{1,...,n\}$, $\mathcal{E}=\mathcal{N}\times\mathcal{N}$, and $\mathbf{A}=[a_{ij}]\in\mathbb{R}^{n\times n}$ (square real matrix) are its node set, edge set, and adjacency matrix, respectively. If node i and node j can exchange data, then they are neighbors (adjacents), $(i,j)\in\mathcal{E}$, and $a_{ij}>0$; otherwise, they are not neighbors, $(i,j)\notin\mathcal{E}$, and $a_{ij}=0$. Let $N_i=\{j\mid(i,j)\in\mathcal{E}\}$ and $d_i=\sum_{j\in N_i}a_{ij}$ be the neighbor set and in-degree of node i, respectively. Laplacian matrix of $\mathcal{G}$ is $\mathbf{L}=\mathbf{D}-\mathbf{A}$, where, $\mathbf{D}=diag\{d_i\}$ (proper diagonal matrix). A path from node i to node j is a sequence of pairs, belong to $\mathcal{E}$, expressed as $\{(i,n_1),...,(n_m,j)\}$. A graph is connected, if there exists a path between any two distinct nodes within the graph [35].

B. Droop-Controlled Inverter-Interfaced DG

In autonomous MGs, voltage-controlled inverter-based DGs are responsible to construct the grid's voltage waveform. In order to accomplish control objectives in different levels, these

grid-forming DGs are preferably controlled in a hierarchical manner [36]. Zero level comprises the most inner loops, controlling the inverter's output voltage and current. For a DG,

- There exist various types of zero-level controllers, not an unique general type [37], [38].
- The subsystem, comprising zero-level controllers, inverter, and LC filter, has a high bandwidth [37], [38].

Therefore, in secondary control studies, generally one can consider the following model for i^{th} DG [1].

$$\dot{\delta}_i = 2\pi f_i, \tag{1a}$$
$$\tau_i^V \dot{V}_i = -V_i + V_i^*, \tag{1b}$$

where, the frequency f_i is converted to the phase angle δ_i instantaneously and the voltage V_i tracks its desire V_i^* with the delay τ_i^V.

Unlike the conventional synchronous generators (SGs), there is no inherent relationship between inverter's output frequency and power. For dominantly inductive (actual or virtual) MGs, active and reactive powers are mainly influenced by frequency and voltage, respectively. Accordingly, the droop control equations, emulating SGs behavior, are [1]

$$f_i = f_{nom} - m_i P_i^m + \Omega_i, \tag{2a}$$
$$V_i^* = V_{nom} - n_i Q_i^m, \tag{2b}$$

where, $m_i = \Delta f_{max}/P_i^*$, $n_i = \Delta V_{max}/Q_i^*$ are droop coefficients; Δf_{max} and ΔV_{max} are the maximum allowable frequency and voltage deviations; P_i^* and Q_i^* are i^{th} DG's active and reactive power capacities; V_{nom}, f_{nom} are nominal voltage and frequency; Ω_i is i^{th} DG's frequency correction term to be defined later; P_i^m, Q_i^m are the measured active and reactive powers by using the low-pass filters below.

$$\tau_i^{LP} \dot{P}_i^m = -P_i^m + P_i, \tag{3a}$$
$$\tau_i^{LP} \dot{Q}_i^m = -Q_i^m + Q_i, \tag{3b}$$

where, $\tau_i^{LP} = (2\pi f_i^c)^{-1}$ is the low-pass filter's time constant and f_i^c is its cutoff frequency; P_i, Q_i are active and reactive powers of i^{th} DG.

C. Microgrid Electrical Network

Following the classical power system studies, it is assumed that the loads and feeder lines are modeled by constant impedances (admittances) [39]. Thus, applying the well-known Kirchhoff's laws to the resultant admittance network, one can obtain a set of nonlinear algebraic equations [40]. The dimension of this set of equations can be reduced to the number of DGs, by using the Kron reduction method [40], [41]. Suppose that in the Kron-reduced network, the DGs i and j are interconnected via the admittance $Y_{ij} = G_{ij} + jB_{ij} \in \mathbb{C}$, where $G_{ij} \in \mathbb{R}$ and $B_{ij} \in \mathbb{R}$ are conductance and susceptance, respectively. Therefore, one can write i^{th} DG's output powers in the power-flow equations format as follows [1], [40].

$$P_i = G_i V_i^2 + \sum\nolimits_j V_i V_j G_{ij} \cos(\delta_i - \delta_j) + \sum\nolimits_j V_i V_j B_{ij} \sin(\delta_i - \delta_j), \tag{4a}$$
$$Q_i = -B_i V_i^2 - \sum\nolimits_j V_i V_j B_{ij} \cos(\delta_i - \delta_j) + \sum\nolimits_j V_i V_j G_{ij} \sin(\delta_i - \delta_j), \tag{4b}$$

where, $G_i = G_{ii} + \sum_j G_{ij}$, $B_i = B_{ii} + \sum_j B_{ij}$; $G_{ii} \in \mathbb{R}$ (resp. $B_{ii} \in \mathbb{R}$) is i^{th} DG's shunt conductance (resp. susceptance).

Remark 1: Conditions for the stability of the droop-controlled MGs has been already investigated in the literature [1], [17], [19]. According to (2a), if $\Omega_i = 0$, the droop control leads to steady-state frequency deviations equal to $m_i P_i = m_j P_j, \forall i, j$, implying proportional load-sharing. The frequency deviations may hamper the performance of the system and deviate out from the allowable range [3]; hence, they should be compensated by using the secondary term Ω_i.

III. Secondary Hz-Watt Control

A. Conventional Approaches

In the previous works, to compensate for the droop-induced frequency deviations, a PI-based correction term with the following general form has been proposed.

$$\Omega_i = K_p \epsilon_i + K_i \int \epsilon_i dt, \tag{5}$$

where, K_p, K_i are proportional, integral gains; ϵ_i denotes the error to be reduced. Thus far, a variety of errors and PI gains has been proposed (utilized) in the conventional secondary controllers. Generally speaking, these errors are all considered to meet two steady-state objectives: *i)* $f_i = f_{nom}, \forall i$, i.e., zero frequency error, and *ii)* $\Omega_i = \Omega_j$ or $m_i P_i = m_j P_j, \forall i, j$, i.e., proportional power-sharing. For instance, in [7], [31] the error in (5) is in a consensus-based form as

$$\epsilon_i = g_i^f [\sum\nolimits_j a_{ij}(f_j - f_i) + b_i(f_{nom} - f_i)] + g_i^P \sum\nolimits_j a_{ij}(m_j P_j - m_i P_i), \tag{6}$$

where, g_i^f, g_i^P are positive feedback gains; if i^{th} DG can access f_{nom}, then $b_i = 1$, and $b_i = 0$ otherwise; a_{ij} is a communication link weighting defined in Section II-A. Note that the controller in [31] is event-triggered; hence in (6) the sampled signals of f_i, f_j and $m_i P_i$, $m_j P_j$ are employed.

B. Instantaneous Frequency Restoration

The secondary controllers, based on the PI compensation in (5), introduce an extra state Ω_i to each DG's dynamics. This state, which is the frequency correction term, requires a differential equation to be solved. In addition, according to (1a) and (2a), each DG has an integrator in its frequency control loop, per se. Therefore, to remove the extra PI-based compensation in (5) and to benefit from the intrinsical integrator in (1a), the correction term in (7) is proposed. This term is inspired by the consensus algorithm in [34] and denotes the *weighted average of neighboring DGs' frequency deviations*, i.e., $m_j P_j^m, \forall j \in N_i$.

$$\Omega_i = \frac{1}{d_i} \sum\nolimits_{j \in N_i} a_{ij} m_j P_j^m, \tag{7}$$

where, a_{ij}, N_i, and $d_i \neq 0$ are defined in Section II-A. According to (7), the proposed correction term involves *algebraic operations* rather than differential operations; thus, it is computed *instantaneously*.

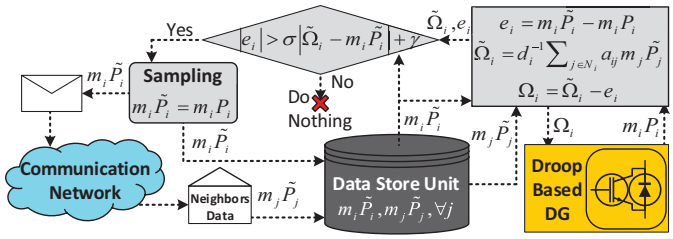

Fig. 2. Schematic diagram of the proposed secondary Hz-Watt controller with event-triggered data exchange, decribed in Algorithm 1.

C. Event-Triggered Data Exchange

The correction term in (7) requires the i^{th} DG to monitor the continuous-time signals of its neighbors $m_jP_j^m$ to perform the instantaneous averaging action. This requirement can be met by conventional periodic signal transmission strategies. However, in order to achieve a good performance, the continuous controller (7) needs a high bandwidth data network to be implemented. On the other hand, in the Hz-Watt control task, all the signal samplings in the periodic strategies may not be necessary, particularly in steady state when the frequency is well-regulated and the powers are properly shared. Therefore, proposing a method which utilizes an aperiodic data exchange strategy seems to be effective for reducing the communication burden (the number of information exchanges). To this end, the event-triggered control strategy provides a good solution, under which the local signals are sampled and broadcasted at each DG's own triggering instants. In this way, the correction term in (7) can be modified to (8), which is computed based on the latest sampled information of DGs, i.e., $m_i\tilde{P}_i^m, \forall i$.

$$\Omega_i = \tilde{\Omega}_i - e_i, \quad \text{where} \begin{cases} \tilde{\Omega}_i = \frac{1}{d_i}\sum_{j\in N_i} a_{ij}m_j\tilde{P}_j^m, \\ e_i = m_i\tilde{P}_i^m - m_iP_i^m. \end{cases} \tag{8}$$

At any time t, the latest sampled information are

$$\begin{cases} m_i\tilde{P}_i^m(t) = m_iP_i^m(t_{k_i}^i) & t \in [t_{k_i}^i, t_{k_i+1}^i), \\ m_j\tilde{P}_j^m(t) = m_jP_j^m(t_{k_j}^j) & t \in [t_{k_j}^j, t_{k_j+1}^j), \end{cases} \tag{9}$$

where, $t_0^i, t_1^i, \cdots$ are triggering instants of i^{th} DG, corresponding to a set of triggering conditions. In other words, each triggering instant is the time when a condition is satisfied. In (8), instead of $m_iP_i^m$ and $m_jP_j^m$, the piece-wise constant signals in (9) are employed; thus, the triggering condition should be designed to control the error e_i. Accordingly, the proposed event-triggering condition is

$$|e_i| > \sigma|\tilde{\Omega}_i - m_i\tilde{P}_i| + \gamma, \tag{10}$$

where, $\sigma \leq 0.5$ and γ are non-negative constants. Note that, once (10) is met, an event is detected; hence, i^{th} DG does sample the data $m_i\tilde{P}_i = m_iP_i$ and broadcasts it to the adjacent DGs. Moreover, the latest received neighbors' information $m_j\tilde{P}_j, \forall j \in N_i$, are all stored in a local data store unit (DSU) and the correction term Ω_i is then computed based on them. Fig. 2 depicts the schematic diagram of the described method. Stability, equilibrium, and Zeno-freeness analyses of the MG under the event-triggered control are presented in Appendix A.

Algorithm 1 The proposed event-triggering algorithm.

initialization: ▷ The first triggering instant t_0^i
Sample $m_i\tilde{P}_i \leftarrow m_iP_i$
Store the sample in the Data Store Unit
Send $m_i\tilde{P}_i$ to other DGs
Compute $\tilde{\Omega}_i$, e_i, Ω_i in (8)
while Hz-Watt control is active **do**
  Compute $e_i = m_i\tilde{P}_i - m_iP_i$
  Alert the data receiver
  if (10) holds **then** ▷ Triggers
    Do lines 1 to 3 of the algorithm
  end if
  for all $j \in N_i$ **do**
    if new data received **then** ▷ Data receive
      Update and store $m_j\tilde{P}_j$ in the Data Store Unit
    end if
  end for
  Do line 4 of the algorithm
end while

D. Requirements and Design Guidelines

In what follows, the readers are provided with some requirements and guidelines for designing the proposed Hz-Watt control in (7) or (8)-(10), based on the upcoming theoretical analyses in Appendix A.

- ***Stability:*** Firstly, the matrix $\mathcal{A}$ in (15) must be Hurwitz, i.e., its eigenvalues have non-positive real parts. This can be investigated by using Schur-complement determinant formula. Secondly, the MG must has stable and bounded voltage dynamics and finite model uncertainties such that in (15) one has $|\boldsymbol{\varphi}| < \varphi_{max}\mathbf{1}_{2n}$. Thirdly, the parameter σ must be selected as $\sigma < 0.5$.
- ***Desired equilibrium:*** The communication network graph must be connected.
- ***Zeno-freeness:*** According to (25), $\gamma \neq 0$ results in nonzero inter-event time intervals.
- ***Parameter selection:*** According to (25), to increase the interval between consecutive communication instants the parameters $\sigma < 0.5$ & γ should be selected as large as possible. On the other hand, from (22) one can see that the parameter γ determines the steady-state Hz-Watt control accuracy. Taking the mentioned trade off into account and considering 2γ as the maximum steady-state frequency variation, one should select proper γ.

IV. Case Studies

A 220-V, 50-Hz MG, consisting of four DGs, is simulated in MATLAB/SimPowerSystems software environment. Each DG feeds a local bus through a feeder line. The local buses are all connected to a common bus (load) via their respective lines. Fig. 3 indicates the single-line diagram of the test MG, where its electrical, control, and communication specification are given, as well. Any transmission line is modeled by a lumped RL impedance. Each 3-phase load is considered as a series RL branch. Note that cutoff frequencies of the power measurement low-pass filters are 5-Hz.

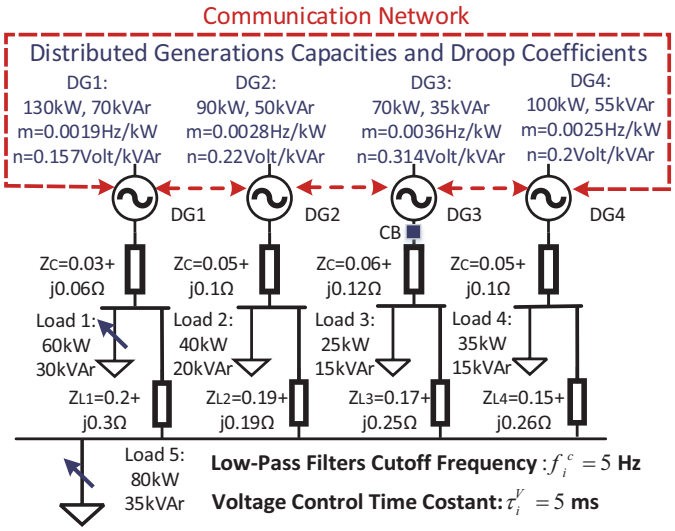

Fig. 3. The test microgrid system and its specifications. The communication links are depicted by dashed lines.

Remark 2: Herein, the inverters and their inner control loops are modeled as (1) for theoretical analyses and controller design. However, the structure of DGs including inverters, PWM mechanisms, LC filters, inner current & voltage controllers, etc. are simulated in detail, in MATLAB/SimPowerSystems environment. The information on the design of this structure and different zero-level controllers are provided in [37].

A. Performance Assessment

Fig. 4 indicates the performance of the proposed controller. The adjacency matrix, of the utilized communication network and the parameters required in (7)-(8) are as follows.

$$[a_{ij}] = \begin{bmatrix} 0 & 1 & 0 & 1 \\ 1 & 0 & 1 & 0 \\ 0 & 1 & 0 & 1 \\ 1 & 0 & 1 & 0 \end{bmatrix}, \quad \begin{cases} \sigma = 0.49, \\ \gamma = 0.0005. \end{cases}$$

According to Fig. 4(a)-(b), prior to $t = 2s$ the MG is engaged with droop-control; thus, the DGs' active powers are shared properly but their frequencies are deviated from the nominal value. After the controller's activation at $t = 2s$, the frequencies are restored to 50-Hz without disturbing the droop-induced power sharing. At $t = 4s$, load 5 becomes 1.5 times greater and it is restored back to the initial value at $t = 7s$. At $t = 7s$, load 1 gets disconnected and gets connected at $t = 10s$. It is shown that, after these load changes, DGs' frequencies are restored to the nominal value, while the active powers are shared properly i.e., $m_i P_i = m_j P_j, \forall i, j$. The second load change at $t = 7s$ happens when the communication link between DGs 1 & 2 is interrupted. This underlines the resiliency of the proposed method to link failures.

Fig. 4(c) indicates the event (communication) instants associated with DGs. At $t = 2s$, the controller is activated and all the DGs, exchange their frequency deviations i.e., $m_i P_i$s with their neighbors; hence, the frequency is restored to 50-Hz. This frequency restoration does not affect active power sharing significantly such that the threshold in (10) is not violated and no more communication is needed. It is shown that most of the data exchanges occur during the transient stages (e.g., load changes), not over the steady-state stages. Thus, many redundant communications are avoided through the proposed need-based communication strategy. Moreover, it is obvious that the time interval between consecutive event times is positive; i.e., the Zeno behavior does not happen.

B. Plug-and-Play Capability Verification

All the requirements (matrix and parameters) are similar to those used in the former subsection. Fig. 5 indicates the performance of the controller for 3rd DG's PnP functionality. At $t = 13s$, the circuit breaker (CB) is intentionally opened, 3rd DG becomes disconnected, and its corresponding communication links are all interrupted. At $t = 16s$, the CB is closed again, the DG returns to the MG, and its communication links are all recovered. It is shown that once 3rd DG leaves the MG, *i*) other DGs increase their supplied active powers proportional to their rated capacities and try to maintain their frequencies at 50-Hz, and *ii*) 3rd DG does not communicate anymore, while other DGs communicate more frequently until the frequency regulation and active power sharing is achieved. In addition, it is shown that once 3rd DG joins the MG again, *i*) immediately participates in frequency/active power control, and *ii*) like other DGs, increases its communications until the control goal is achieved again.

C. Assessment of the Communication Delays Effects

In this subsection, the impacts of communication delays on the system's performance is investigated. The required adjacency matrix and parameteres are same as the ones used in the former cases. The communication delays in practical communication infrastructures are in the order of tens of milliseconds [31]. However, performance of the proposed controller in the presence of the delays of $0.2s$ and $0.35s$ is depicted in Fig. 6. Prior to $t = 4s$, load 5 is $160\text{kW}+j70\text{kVAr}$. At $t = 4s$ and $t = 7s$, load 5 experiences decrease and increase of $80\text{kW}+j35\text{kVAr}$, respectively. At $t = 11s$, 3rd DG leaves the MG and returns back to the MG at $t = 15s$. It is shown that the communication delays deteriorate the transient performance of the system and result in bounded oscillations in the frequencies and supplied active powers. However, f_is and $m_i P_i$s can achieve steady-state agreement, even in the presence of the communication delays of $0.2s$ and $0.35s$.

D. Evaluation of the Impacts of γ on the System Performance

Herein, the scenario in SectionIV-A is re-simulated with different values of γ. Fig. 7 illustrates the DGs' frequency responses over $t \in [4s, 7s]$, i.e., after increase of load 5 at $t = 4s$. One can see that the frequencies have some variations around 50-Hz with the maximum error of the given 2γ. This finding coincides with the equilibrium analyses in Appendix A. That is, the more γ, the less accurate frequency regulation.

Although reducing γ leads to more accurate frequency regulation, it may result in lower inter-event time intervals and hence a huge number of communications, in particular

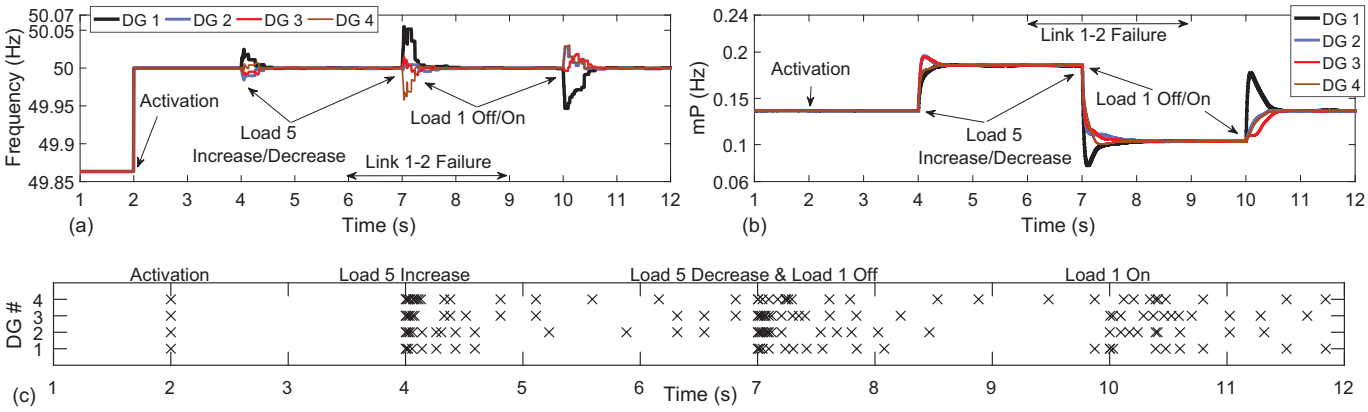

Fig. 4. Performance of the proposed controller after activation, load disturbances, and link failure; (a) frequencies, (b) m_iP_is, and (c) communication instants.

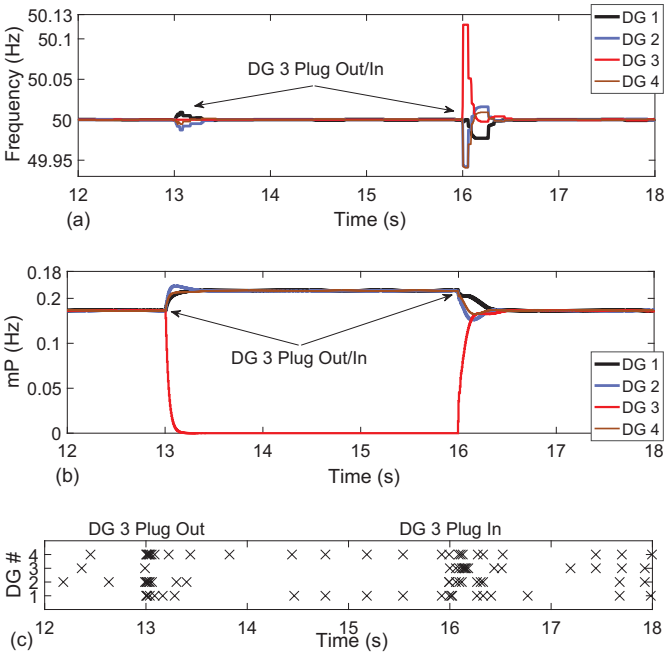

Fig. 5. Plug-and-play performance of 3rd DG; (a) frequencies, (b) m_iP_is, and (c) communication instants.

in steady state. To investigate this trade off, the number of communications executed by each DG for the three cases in Fig. 7 are recorded and the results are given in Fig. 8. Note that these communications only are those executed during $t \in [4s, 7s]$ in Fig. 7. According to Fig. 8, utilizing a $\gamma \neq 0$ reduces the communication burden, significantly. All these findings validate the parameter selection in Section III-D.

E. Comparison with Conventional Approaches

In this subsection, regarding the contributions of this paper the proposed method is compared with the conventional ones in two aspects. First, the scenario in Section IV-A is re-simulated with both the continuous-time correction terms (5) and (7). To make a fair comparison, similar to the work in this paper, it is assumed that all the DGs can access f_{nom} directly; hence, the the controller described by (5)-(6) (utilized in [7], [31]) is modified and employed as

$$\Omega_i = \int g_i^f (f_{nom} - f_i) + g_i^P \sum_j a_{ij}(m_j P_j - m_i P_i) dt, \quad (11)$$

where, $g_i^f = 10$, $g_i^P = 5$ and the same communication network is used. The simulation results associated with 3rd DG under the methods are given in Fig. 9. According to Fig. 9(b), both methods lead to almost similar power responses i.e., m_3P_3. However, from Fig. 9(a) one can see that the proposed method compensates for the frequency deviation instantaneously.

On top of the foregoing comparison, the proposed event-triggered Hz-Watt control is compared with its time-triggered version and the one in [31], in terms of their communication pattern & burden. To this end, the controller (11) is augmented with the event-triggering mechanism proposed in [31]. In addition, the proposed controller in (7) is implemented via a periodic data transmission strategy with the communication frequency of 25-Hz. The scenario in Section IV-A is repeated with the above described approaches, and the communication instants of 3rd DG & the number of communications of all the DGs are summarized in Fig. 10 & Fig. 11, respectively.

According to Fig. 10, compared to the other methods most of the communications under the proposed method are executed during transient stages and the steady-state data exchanges are highly reduced. This underlines that the proposed communication strategy is need-based. To know how much this need-based strategy reduces the communication burden, the number of communications over a period of time should be considered. Fig. 11 depicts the DGs' number of communications for different approaches over $t \in [4s, 12s]$. Accordingly, the proposed method needs dramatically less communications than the method in [31]; even less than the number of communications under the periodic strategy. The average number of communications under the proposed method for DGs 1 to 4 are 5.88, 13.6, 11, and 10.25, respectively (obtained via dividing the communication numbers by the time duration i.e., $12s - 4s = 8s$). Looking at Fig. 10, one can see that these averages for time intervals containing longer steady-state duration will be smaller.

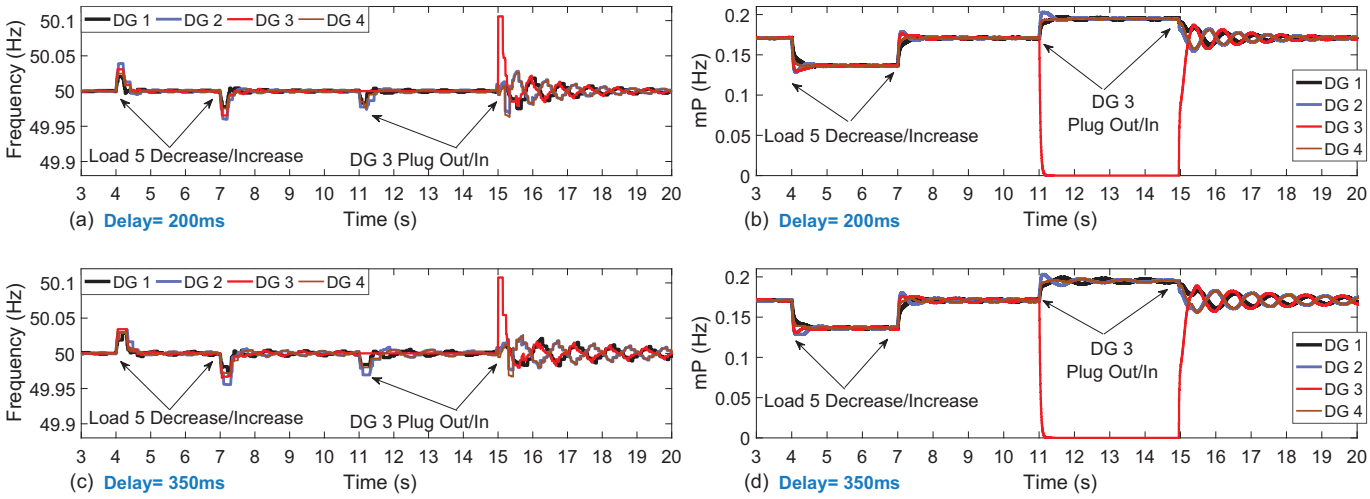

Fig. 6. Impacts of communication delays on the performance of the proposed control scheme; (a)-(b) delays of $0.2s$ and (c)-(d) delays of $0.35s$.

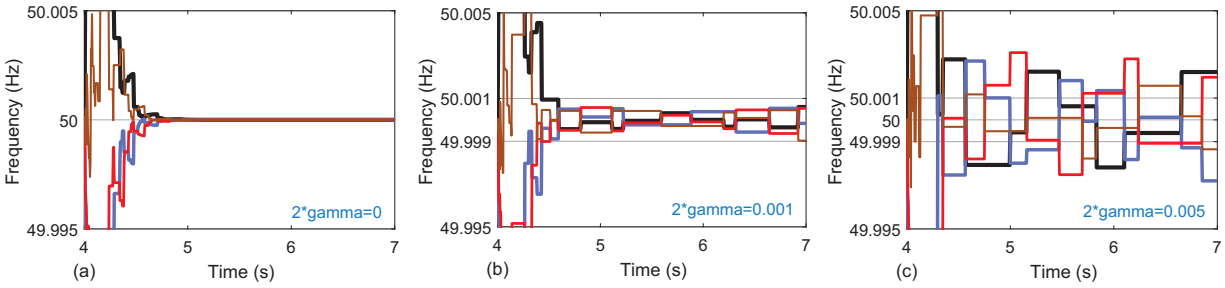

Fig. 7. Impact of γ (gamma) on the steady-state frequency errors after the load change at $t = 4s$ in Fig. 4; (a) $\gamma = 0$, (b) $\gamma = 0.001/2$, and (c) $\gamma = 0.005/2$.

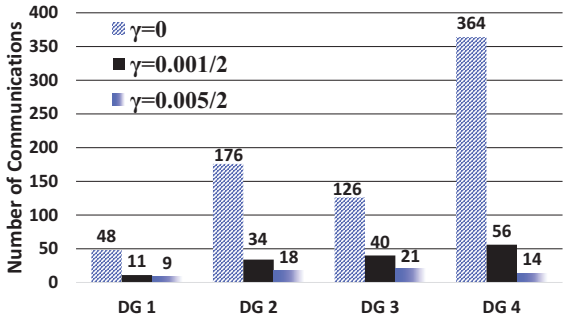

Fig. 8. Impact of γ on the number of communications associated with different DGs for $t \in [4s, 7s]$ in the scenario in Section IV-A. The corresponding frequency respones are depicted in Fig. 7.

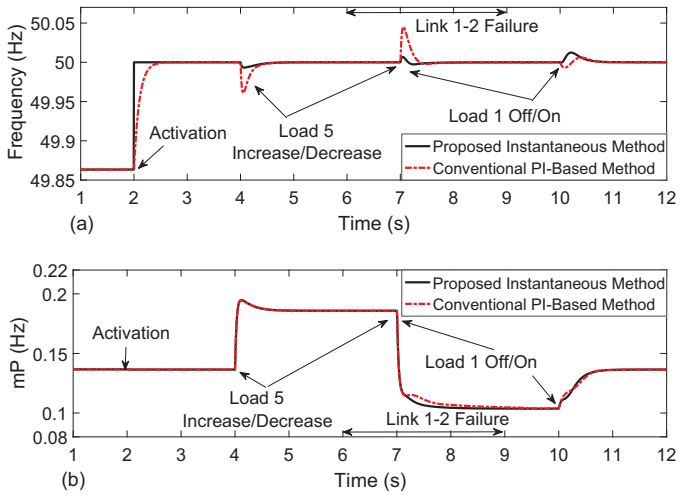

Fig. 9. Performance of 3rd DG under the proposed controller in comparsion with the PI-based method; (a) frequency f_3 and (b) $m_3 P_3$.

V. Conclusion

In this paper, the problem of frequency regulation and proportional active power sharing for islaned inverter-based MGs is solved, simultaneously. In this way, the average of frequency deviations associated with the neighboring DGs is added to each DG's Hz-Watt droop characteristic as an algebraic correction term. Advantages of the method are twofold; *i*) no PI compensation is used to generate the correction terms, and *ii*) the data exchange strategy is need-based. The design points are given and the system's stability, equilibrium, and Zeno-freeness analyses are investigated. Effectiveness of the proposed controller is validated by simulating a test MG for different case studies. Under the presented method the Hz-Watt control task can be achieved, even after experiencing significant load changes, communication time delays and link

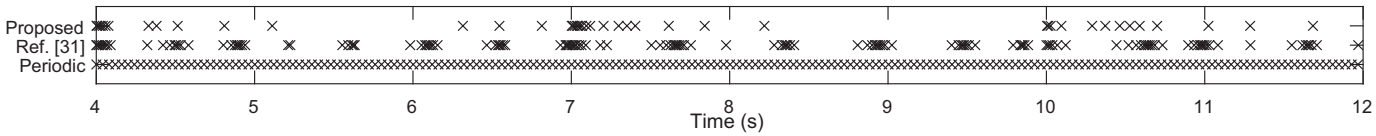

Fig. 10. Communication (event) instants of 3rd DG under different approaches; method in Section III-C vs method in [31] vs method in Section III-B with periodic communications (25-Hz).

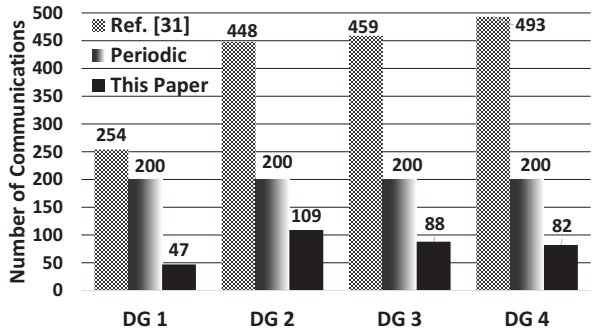

Fig. 11. The number of communications associated with different DGs for $t \in [4s, 12s]$ under different data exchange strategies. The corresponding communication instants are depicted in Fig. 10.

failure, and DG's disconnection/connection. Furthermore, the advantages of the proposed method over the conventional approaches are highlighted in a comparative study.

APPENDIX A

In order to analyze the Hz-Watt stability, the state model of the whole MG is required. One can write (1)-(3), and (8) in the following compact form.

$$\begin{aligned}\dot{\boldsymbol{\delta}} &= -2\pi\mathbf{D}^{-1}\mathbf{L}(\mathbf{m}\tilde{\mathbf{P}}_m) + 2\pi f_{nom}\mathbf{1}_n \\ &= -2\pi\mathbf{D}^{-1}\mathbf{L}(\mathbf{m}\mathbf{P}_m) - 2\pi\mathbf{D}^{-1}\mathbf{L}\mathbf{e} + 2\pi f_{nom}\mathbf{1}_n, &(12a)\\ \dot{\mathbf{P}}_m &= -\boldsymbol{\tau}_{LP}^{-1}\mathbf{P}_m + \boldsymbol{\tau}_{LP}^{-1}\mathbf{P}, &(12b)\\ \dot{\mathbf{V}} &= -\boldsymbol{\tau}_V^{-1}\mathbf{V} - \boldsymbol{\tau}_V^{-1}\mathbf{n}\mathbf{Q}_m + V_{nom}\boldsymbol{\tau}_V^{-1}\mathbf{1}_n, &(12c)\\ \dot{\mathbf{Q}}_m &= -\boldsymbol{\tau}_{LP}^{-1}\mathbf{Q}_m + \boldsymbol{\tau}_{LP}^{-1}\mathbf{Q}, &(12d)\end{aligned}$$

where, $\mathbf{e} = \mathbf{m}\tilde{\mathbf{P}}_m - \mathbf{m}\mathbf{P}_m$; $\forall i\ \mathbf{1}_n = \text{col}\{1\}$, $\boldsymbol{\delta} = \text{col}\{\delta_i\}$, $\mathbf{V} = \text{col}\{V_i\}$, $\mathbf{P}_m = \text{col}\{P_i^m\}$, $\tilde{\mathbf{P}}_m = \text{col}\{\tilde{P}_i^m\}$, $\mathbf{Q}_m = \text{col}\{Q_i^m\}$, $\mathbf{P} = \text{col}\{P_i\}$, and $\mathbf{Q} = \text{col}\{Q_i\}$ are state column vectors; $\boldsymbol{\tau}_V = \text{diag}\{\tau_i^V\}$, $\boldsymbol{\tau}_{LP} = \text{diag}\{\tau_i^{LP}\}$, $\mathbf{m} = \text{diag}\{m_i\}$ and $\mathbf{n} = \text{diag}\{n_i\}$ are proper diagonal matrices.

Stability analysis: The MG model in (4) can be written as

$$\mathbf{P} = \mathbf{F}_P(\boldsymbol{\delta}, \mathbf{V}), \quad (13a)$$
$$\mathbf{Q} = \mathbf{F}_Q(\boldsymbol{\delta}, \mathbf{V}), \quad (13b)$$

where, $\mathbf{F}_P$, $\mathbf{F}_Q : \mathbb{R}^{n\times n} \to \mathbb{R}^n$ are some nonlinear functions.

In order to keep the system stability and to avoid some power quality issues, in comparison with the distribution system standards (e.g., IEEE 1547), the MGs bus voltage drifts should be smaller [14]. To this end, in practice the voltages are contained in a reasonable range around the nominal value, by using proper droop coefficients $n_i = \Delta V_{max}/Q_i^*$ or a voltage controller [14], or by saturating the voltages [20]. Therefore, without the loss of generality, by replacing the voltages in (4a) with nominal voltage and considering small voltage angle differences one can write

$$\mathbf{P} = V_n^2\mathbf{L}_B\boldsymbol{\delta} + \underbrace{V_n^2(2\mathbf{G_i} - \mathbf{G_{ii}})}_{\mathbf{P}_V} + \boldsymbol{\varphi}_m, \quad (14)$$

where, the model uncertainties as well as the effects of voltage variations on the Hz-Watt dynamics are represented by $\boldsymbol{\varphi}_m$ as a disturbance vector; $\mathbf{G_i} = \text{col}\{G_i\}$ and $\mathbf{G_{ii}} = \text{col}\{G_{ii}\}$ are the vectors of conductances; $\mathbf{P}_V$ denotes a constant voltage-dependent active power demand (say nominal demand) [40]; $\mathbf{L}_B$ denotes the Laplacian matrix of the MG electric network with $\mathbf{B} = [B_{ij}] \in \mathbb{R}^n$ being its associated adjacency matrix (see Section II-A for more info). From (12) and (14) one has the following state model with the state vector $\mathbf{x} = [\boldsymbol{\delta}^T, \mathbf{P}_m^T]^T$.

$$\dot{\mathbf{x}} = \mathcal{A}\mathbf{x} + \mathbf{u}, \text{ where } \mathbf{u} = \boldsymbol{\varphi} + \begin{bmatrix} -2\pi\mathbf{D}^{-1}\mathbf{L}\mathbf{e} \\ \mathbf{0}_n \end{bmatrix}, \quad (15)$$

$$\boldsymbol{\varphi} = \begin{bmatrix} 2\pi f_{nom}\mathbf{1}_n \\ \boldsymbol{\tau}_{LP}^{-1}(\mathbf{P}_V + \boldsymbol{\varphi}_m) \end{bmatrix}, \mathcal{A} = \begin{bmatrix} \mathbf{0}_n & -2\pi\mathbf{D}^{-1}\mathbf{L}\mathbf{m} \\ V_n^2\boldsymbol{\tau}_{LP}^{-1}\mathbf{L}_B & -\boldsymbol{\tau}_{LP}^{-1} \end{bmatrix};$$

$\mathbf{0}_n$ is a vector of zeros; $\boldsymbol{\varphi}$ is considered as a disturbance vector. Under the triggering condition (9) one always has $|e_i| \le \sigma|\tilde{\Omega}_i - m_i\tilde{P}_i| + \gamma$ and hence

$$|\mathbf{e}| \le \sigma|\mathbf{D}^{-1}\mathbf{L}(\mathbf{m}\mathbf{P}_m + \mathbf{e})| + \gamma\mathbf{1}_n, \quad (16)$$

where, $|\cdot|$ denotes the entry-wise absolute value matrix/vector; i.e., $|\mathfrak{M}| = [|\mathfrak{m}_{ij}|], \forall\mathfrak{M} = [\mathfrak{m}_{ij}]$. According to the well-known triangle inequality, one can bound (16) as

$$|\mathbf{e}| \le \sigma|\mathbf{D}^{-1}\mathbf{L}\mathbf{m}||\mathbf{P}_m| + \sigma|\mathbf{D}^{-1}\mathbf{L}||\mathbf{e}| + \gamma\mathbf{1}_n. \quad (17)$$

Let's define the matrix $\mathbf{M} = \mathbf{I}_n - \sigma|\mathbf{D}^{-1}\mathbf{L}|$ with $\mathbf{I}_n$ being proper identity matrix. Since $\mathbf{L} = \mathbf{D} - \mathbf{A}$, one has $|\mathbf{D}^{-1}\mathbf{L}| = \mathbf{I}_n + \mathbf{D}^{-1}\mathbf{A}$; hence $\mathbf{M} = (1-\sigma)\mathbf{I}_n - \sigma\mathbf{D}^{-1}\mathbf{A}$. According to the Geršgorian discs theorem [42], if $\sigma < \frac{1}{2}$, then the eigenvalues of $\mathbf{M}$ all have strictly positive real parts. Hence, from Theorem 5.1.4 in [43] $\mathbf{M}$ is invertible and one can write (17) as

$$|\mathbf{e}| \le \mathbf{N}_1|\mathbf{P}_m| + \mathbf{N}_2, \text{ where } \begin{cases}\mathbf{N}_1 = \sigma\mathbf{M}^{-1}|\mathbf{D}^{-1}\mathbf{L}\mathbf{m}|, \\ \mathbf{N}_2 = \gamma\mathbf{M}^{-1}\mathbf{1}_n.\end{cases} \quad (18)$$

According to (15), (18), and the well-known triangle inequality, if $\boldsymbol{\varphi} < \varphi_{max}\mathbf{1}_{2n}$ one then has

$$|\mathbf{u}| < |\mathbf{T}_1||\mathbf{x}| + |\mathbf{T}_2|, \text{ where } |\mathbf{x}| = \begin{bmatrix} |\boldsymbol{\delta}| \\ |\mathbf{P}_m| \end{bmatrix}, \quad (19)$$

$$\mathbf{T}_1 = \begin{bmatrix} \mathbf{0}_n & 2\pi|\mathbf{D}^{-1}\mathbf{L}|\mathbf{N}_1 \\ \mathbf{0}_n & \mathbf{0}_n \end{bmatrix},$$

$$\mathbf{T}_2 = \begin{bmatrix} \varphi_{max}\mathbf{1}_n + 2\pi|\mathbf{D}^{-1}\mathbf{L}|\mathbf{N}_2 \\ \varphi_{max}\mathbf{1}_n \end{bmatrix}.$$

The system (15) and the inequality (19) correspond to Eq. (28) and the inequality (29) in [44], respectively. Therefore, if

the matrix $\mathcal{A}$ is Hurwitz, then the bounded stability analysis follows the results of Theorem 2 in [44]; i.e., the solutions of the system (15) are ultimately uniformly bounded (UUB). The notion of UUB-ness as well as the systematic approach for calculating the states' bounds is available in [44].

According to the performed analysis, the system stability ows to the boundedness of the vector $\boldsymbol{\varphi}$, i.e., $|\boldsymbol{\varphi}| < \varphi_{max}\mathbf{1}_{2n}$, and positivity of the real parts of eigenvalues of the matrix $\mathcal{A}$. The former is guaranteed, if the microgrid's voltage controller is stable, the voltages are well-regulated around the nominal voltage, and the MG system has finite model uncertainties. The latter, can be investigated by using the Schur-complement determinant formula, similar to the work done in Section V-A of [16] for secondary voltage control. ■

Equilibrium analysis: Frequency is a global valid entity across the MG being similar for all the DGs in steady state, i.e., $\dot{\delta}_i = 2\pi f_{MG}$. Moreover, in steady state one has $P_i^m = P_i$; hence, from (12a)-(12b) one can write

$$(f_{MG} - f_{nom})\mathbf{1}_n + \mathbf{D}^{-1}\mathbf{L}(\mathbf{m}\tilde{\mathbf{P}}_m) = \mathbf{0}_n. \tag{20}$$

Equation (20) corresponds to the Eq. (8) in [18]. If the communication graph between the DGs is *connected*, then the convergence (equilibrium) point analysis follows the results of Theorem 2 in [18], i.e., $f_i = f_{nom}$ & $m_i\tilde{P}_i = m_j\tilde{P}_j, \forall i,j$. On the other hand, according to (8) one can write

$$|m_iP_i^m - \frac{1}{d_i}\sum\nolimits_{j\in N_i} a_{ij}m_jP_j^m| \le |e_i| + \frac{1}{d_i}\sum\nolimits_{j\in N_i} a_{ij}|e_j| + |\tilde{\Omega}_i - m_i\tilde{P}_i|. \tag{21}$$

In steady state $\forall i,j$ one can write $m_i\tilde{P}_i = m_j\tilde{P}_j$, $P_i^m = P_i$, and $|e_i| \le \sigma|\tilde{\Omega}_i - m_i\tilde{P}_i| + \gamma$; hence, from (8) & (21) one has

$$|m_iP_i - \frac{1}{d_i}\sum\nolimits_{j\in N_i} a_{ij}m_jP_j| \le 2\gamma. \tag{22}$$

The last inequality indicates that each DG's data m_iP_i differs from the average of its neighbors' data with a maximum error of 2γ. In other words, under the proposed event-triggered controller the DGs' active powers are shared properly but with a controllable steady-state error. In addition, according to (2a) & (8) the above error can be translated into the steady-state frequency regulation error with the maximum value of 2γ. ■

Remark 3: The above stability and equilibrium analyses are associated with the event-triggered controller in (8). However, to investigate the stability of the system under the continuous-time controller in (7) one can easily set $\mathbf{e} = \mathbf{0}_n$ in (12a) and then follow the same procedure.

Zeno-freeness analysis: Consider the function $y_i = |e_i| = |m_i\tilde{P}_i^m - m_iP_i^m|$ over the time interval $[t_{k_i}^i, t_{k_i+1}^i)$, when it is continuous. Differentiating y_i and using (3a) & (9) one has

$$\dot{y}_i = \pm\dot{e}_i \le |\dot{e}_i| \le m_i|\dot{P}_i^m| \le (m_i/\tau_i^{LP})|P_i - P_i^m|. \tag{23}$$

If over the interval $[t_{k_i}^i, t_{k_i+1}^i)$ one has $|P_i - P_i^m| \le \alpha_{k_i}^i$, then considering the initial value $y_i(t_{ki}^i) = 0$ one has

$$y_i \le (m_i\alpha_{k_i}^i/\tau_i^{LP})(t - t_{k_i}^i),\ t \ge t_{k_i}^i, \tag{24}$$

From (10) the next event time, i.e., $t_{k_i+1}^i$ is when $y_i > \sigma|\tilde{\Omega}_i - m_i\tilde{P}_i| + \gamma$; hence, from (24) at that moment one definitely has

$$t_{k_i+1}^i - t_{k_i}^i > \frac{\tau_i^{LP}(\sigma|\tilde{\Omega}_i - m_i\tilde{P}_i| + \gamma)}{m_i\alpha_{k_i}^i}, \tag{25}$$

which underlines that the system is Zeno-free. Furthermore, from (25) one can see that the more the parameters σ, γ, and τ_i^{LP}, the greater the inter-event time-intervals, and the lower number of communications. ■

REFERENCES

[1] J. Schiffer, R. Ortega, A. Astolfi, J. Raisch, and T. Sezi, "Conditions for stability of droop-controlled inverter-based microgrids," *Automatica*, vol. 50, no. 10, pp. 2457–2469, Oct. 2014.

[2] Y. Han, H. Li, P. Shen, E. A. A. Coelho, and J. M. Guerrero, "Review of active and reactive power sharing strategies in hierarchical controlled microgrids," *IEEE Trans. Power Electron.*, vol. 32, no. 3, pp. 2427–2451, Mar. 2017.

[3] J. M. Guerrero, J. C. Vasquez, J. Matas, L. G. de Vicuna, and M. Castilla, "Hierarchical Control of Droop-Controlled AC and DC MicrogridsA General Approach Toward Standardization," *IEEE Trans. Ind. Electron.*, vol. 58, no. 1, pp. 158–172, Jan. 2011.

[4] M. Yazdanian and A. Mehrizi-Sani, "Distributed Control Techniques in Microgrids," *IEEE Trans. Smart Grid*, vol. 5, no. 6, pp. 2901–2909, Nov. 2014.

[5] M. Kosari and S. H. Hosseinian, "Decentralized Reactive Power Sharing and Frequency Restoration in Islanded Microgrid," *IEEE Trans. Power Syst.*, vol. 32, no. 4, pp. 2901–2912, Jul. 2017.

[6] M. Castilla, A. Camacho, J. Miret, M. Velasco, and P. Martí, "Local Secondary Control for Inverter-Based Islanded Microgrids With Accurate Active Power Sharing Under High-Load Conditions," *IEEE Trans. Ind. Electron.*, vol. 66, no. 4, pp. 2529–2539, Apr. 2019.

[7] A. Bidram, A. Davoudi, F. L. Lewis, and Z. Qu, "Secondary control of microgrids based on distributed cooperative control of multi-agent systems," *IET Gener. Transm. Distrib.*, vol. 7, no. 8, pp. 822–831, Aug. 2013.

[8] S. Zuo, A. Davoudi, Y. Song, and F. L. Lewis, "Distributed Finite-Time Voltage and Frequency Restoration in Islanded AC Microgrids," *IEEE Trans. Ind. Electron.*, vol. 63, no. 10, pp. 5988–5997, Oct. 2016.

[9] N. M. Dehkordi, N. Sadati, and M. Hamzeh, "Distributed Robust Finite-Time Secondary Voltage and Frequency Control of Islanded Microgrids," *IEEE Trans. Power Syst.*, vol. 32, no. 5, pp. 3648–3659, Sept. 2017.

[10] Y. Xu and H. Sun, "Distributed Finite-Time Convergence Control of an Islanded Low-Voltage AC Microgrid," *IEEE Trans. Power Syst.*, vol. 33, no. 3, pp. 2339–2348, May. 2018.

[11] N. M. Dehkordi, N. Sadati, and M. Hamzeh, "Fully distributed cooperative secondary frequency and voltage control of islanded microgrids," *IEEE Trans. Energy Convers.*, vol. 32, no. 2, pp. 675–685, Jun. 2017.

[12] X. Wu, C. Shen, and R. Iravani, "A distributed, cooperative frequency and voltage control for microgrids," *IEEE Trans. Smart Grid*, vol. 9, no. 4, pp. 2764–2776, Jul. 2018.

[13] X. Wu and C. Shen, "Distributed optimal control for stability enhancement of microgrids with multiple distributed generators," *IEEE Trans. Power Syst.*, vol. 32, no. 5, pp. 4045–4059, Sept. 2017.

[14] R. Han, L. Meng, G. Ferrari-Trecate, E. A. A. Coelho, J. C. Vasquez, and J. M. Guerrero, "Containment and Consensus-Based Distributed Coordination Control to Achieve Bounded Voltage and Precise Reactive Power Sharing in Islanded AC Microgrids," *IEEE Trans. Ind. Appl.*, vol. 53, no. 6, pp. 5187–5199, Nov/Dec. 2017.

[15] L. Y. Lu and C. C. Chu, "Consensus-based droop control synthesis for multiple DICs in isolated micro-grids," *IEEE Trans. Power Syst.*, vol. 30, no. 5, pp. 2243–2256, Sept. 2015.

[16] J. W. Simpson-Porco, Q. Shafiee, F. Dörfler, J. C. Vasquez, J. M. Guerrero, and F. Bullo, "Secondary frequency and voltage control of islanded microgrids via distributed averaging," *IEEE Trans. Ind. Electron.*, vol. 62, no. 11, pp. 7025–7038, Nov. 2015.

[17] J. W. Simpson-Porco, F. Dörfler, and F. Bullo, "Synchronization and power sharing for droop-controlled inverters in islanded microgrids," *Automatica*, vol. 49, no. 9, pp. 2603–2611, Sept. 2013.

[18] B. Abdolmaleki, Q. Shafiee, and H. Bevrani, "Kron Reduction and L_2-Stability for Plug-and-Play Frequency Control of Microgrids," in *Proc. Smart Grid Conference (SGC)*, Sanandaj, Iran, Nov. 2018.

[19] M. E. Romero and M. M. Seron, "Ultimate Boundedness of Voltage Droop Control with Distributed Secondary Control Loops," *IEEE Trans. Smart Grid*, Early Access, doi: 10.1109/TSG.2018.2849583.

[20] J. Schiffer, T. Seel, J. Raisch, and T. Sezi, "Voltage Stability and Reactive Power Sharing in Inverter-Based Microgrids With Consensus-Based Distributed Voltage Control," *IEEE Trans. Control Syst. Technol.*, vol. 24, no. 1, pp. 96–109, Jan. 2016.

[21] Q. Shafiee, J. M. Guerrero, and J. C. Vasquez, "Distributed Secondary Control for Islanded Microgrids A Novel Approach," *IEEE Trans. Ind. Electron.*, vol. 29, no. 2, pp. 1018–1031, Feb. 2014.

[22] Q. Shafiee, Č. Stefanović, T. Dragičević, P. Popovski, J. C. Vasquez, and J. M. Guerrero, "Robust Networked Control Scheme for Distributed Secondary Control of Islanded Microgrids," *IEEE Trans. Ind. Electron.*, vol. 61, no. 10, pp. 5363–5374, Oct. 2014.

[23] Q. Yang, J. A. Barria, and T. C. Green, "Communication infrastructures for distributed control of power distribution networks," *IEEE Trans. Ind. Informat.*, vol. 7, no. 2, pp. 316–327, May. 2011.

[24] D. Baumann, J. J. Zhu, G. Martius, and S. Trimpe, "Deep reinforcement learning for event-triggered control," in *Proc. 57th IEEE Conference on Decision and Control (CDC)*, Miami, Fl, USA, Dec. 2018, pp. 943–950.

[25] Y. Cheng and V. Ugrinovskii, "Event-triggered leader-following tracking control for multivariable multi-agent systems," *Automatica*, vol. 70, pp. 204–210, Aug. 2016.

[26] L. Ding, Q. L. Han, X. Ge, and X. M. Zhang, "An overview of recent advances in event-triggered consensus of multiagent systems," *IEEE Trans. Cybern.*, vol. 48, no. 4, pp. 1110–1123, Apr. 2018.

[27] E. Garcia, Y. Cao, H. Yu, P. Antsaklis, and D. Casbeer, "Decentralised event-triggered cooperative control with limited communication," *Int. J. of Control*, vol. 86, no. 9, pp. 1479–1488, Sept. 2013.

[28] L. Dong, Y. Tang, H. He, and C. Sun, "An event-triggered approach for load frequency control with supplementary ADP," *IEEE Trans. Power Syst.*, vol. 32, no. 1, pp. 581–589, Jan. 2017.

[29] W. Meng, X. Wang, and S. Liu, "Distributed load sharing of an inverter-based microgrid with reduced communication," *IEEE Trans. Smart Grid*, vol. 9, no. 2, pp. 1354–1364, Mar. 2017.

[30] Y. Fan, G. Hu, and M. Egerstedt, "Distributed reactive power sharing control for microgrids with event-triggered communication," *IEEE Trans. Control Syst. Technol.*, vol. 25, no. 1, pp. 118–128, Jan. 2017.

[31] M. Chen, X. Xiao, and J. M. Guerrero, "Secondary restoration control of islanded microgrids with decentralized event-triggered strategy," *IEEE Trans. Ind. Informat.*, vol. 14, no. 9, pp. 3870–3880, Sept. 2018.

[32] L. Ding, Q. Han, and X. Zhang, "Distributed Secondary Control for Active Power Sharing and Frequency Regulation in Islanded Microgrids Using an Event-triggered Communication Mechanism," *IEEE Trans. Ind. Informat.*, Early Access, doi: 10.1109/TII.2018.2884494.

[33] S. Weng, D. Yue, C. Dou, J. Shi, and C. Huang, "Distributed event-triggered cooperative control for frequency and voltage stability and power sharing in isolated inverter-based microgrid," *IEEE Trans. Cybern.*, vol. 49, no. 4, pp. 1427–1439, Apr. 2019.

[34] J. A. Fax and R. M. Murray, "Information flow and cooperative control of vehicle formations," *IEEE Trans. Autom. Control*, vol. 49, no. 9, pp. 1465–1476, Sept. 2004.

[35] R. Olfati-Saber, J. A. Fax, and R. M. Murray, "Consensus and cooperation in networked multi-agent systems," *Proc. IEEE*, vol. 95, no. 1, pp. 215–233, Jan. 2007.

[36] J. Rocabert, A. Luna, F. Blaabjerg, and P. Rodrguez, "Control of Power Converters in AC Microgrids," *IEEE Trans. Power Electron.*, vol. 27, no. 11, pp. 4734–4749, Nov. 2012.

[37] A. Yazdani and R. Iravani, *Voltage-Sourced Converters in Power Systems: Modeling, Control, and Applications*. John Wiley & Sons, 2010.

[38] T. Dragičević, "Model Predictive Control of Power Converters for Robust and Fast Operation of AC Microgrids," *IEEE Trans. Power Electron.*, vol. 33, no. 7, pp. 6304–6317, Jul. 2018.

[39] P. Varaiya, F. F. Wu, and R.-L. Chen, "Direct methods for transient stability analysis of power systems: Recent results," *Proc. IEEE*, vol. 73, no. 12, pp. 1703–1715, Dec. 1985.

[40] P. Kundur, J. B. Neal, and G. L. Mark, *Power System Stability and Control*. McGraw-Hill Education, 1994.

[41] F. Dörfler and F. Bullo, "Kron Reduction of Graphs With Applications to Electrical Networks," *IEEE Trans. Circuits Syst. I*, vol. 60, no. 1, pp. 150–163, Jan. 2013.

[42] R. A. Horn and C. R. Johnson, *Matrix Analysis*. Cambridge University Press, 2012.

[43] H. Anton and C. Rorres, *Elementary Linear Algebra: Applications Version*, 11th ed. Wiley Global Education, 2013.

[44] E. Kofman, H. Haimovich, and M. M. Seron, "A systematic method to obtain ultimate bounds for perturbed systems," *Int. J. of Control*, vol. 80, no. 2, pp. 167–178, Feb. 2007.

Babak Abdolmaleki (S'17-M'18) is an Invited Researcher at the Smart/Micro Grids Research Center (SMGRC), University of Kurdistan, Sanandaj, Iran. He received his B.S. and M.S. degrees in Electrical Engineering from the Shiraz University, Shiraz, Iran, in 2014 and 2017, respectively.

His main research interests are centered around distributed optimization and control, multi-agent systems cooperation, event-triggered control, advanced control of power converters, and modern power systems dynamics and control.

Qobad Shafiee (S'13-M'15-SM'17) is an Assistant Professor and the Program Co-Leader of the Smart/Micro Grids Research Center (SMGRC) at the University of Kurdistan, Sanandaj, Iran, where he was a Lecturer from 2007 to 2011. He received the Ph.D. degree in Electrical Engineering from the Department of Energy Technology, Aalborg University, Aalborg, Denmark, in 2014. In 2014, he was a Visiting Scholar with the Electrical Engineering Department, University of Texas at Arlington, Arlington, TX, USA. He was a Post-Doctoral Fellow with the Department of Energy Technology, Aalborg University, in 2015.

His current research interests include modeling, energy management, control of power electronics-based systems e.g., microgrids, and model predictive and optimal control of modern power systems.

Mohammad Mehdi Arefi (M'17-SM'17) was born in 1982. He received the B.S. degree from the Department of Electrical Engineering, Shiraz University, Shiraz, Iran, in 2004, and the M.S. and Ph.D. degrees from the Electrical Engineering Department, Iran University of Science and Technology, Tehran, Iran, in 2007 and 2011, respectively. He is an Associate Professor with the Department of Power and Control Engineering, School of Electrical and Computer Engineering, Shiraz University.

His current research interests include adaptive robust control, nonlinear and chaos control, and application of control methods in power systems.

Dr. Arefi is in the editorial board of some journals, including the Iranian Journal of Science and Technology, Transactions of Electrical Engineering, and Industrial Control Magazine.

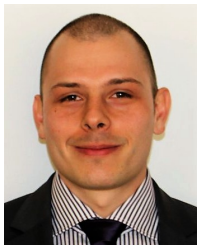

Tomislav Dragičević (S'09-M'13-SM'17) received the M.S. and the industrial Ph.D. degrees in Electrical Engineering from the Faculty of Electrical Engineering, Zagreb, Croatia, in 2009 and 2013, respectively. From 2013 until 2016 he has been a Post-Doctoral Research Associate at the Aalborg University, Denmark. From March 2016 he is an Associate Professor at the Aalborg University where he leads an Advanced Control Lab. He made a Guest Professor stay at the Nottingham University, UK during spring/summer of 2018.

His principal fields of interest are design and control of microgrids, and application of advanced modeling and control concepts to power electronic systems. He has authored and co-authored more than 155 technical papers (more than 70 of them are published in international journals, mostly IEEE Transactions) in his domain of interest, 8 book chapters and a book in the field.

He serves as Associate Editor in IEEE TRANSACTIONS ON INDUSTRIAL ELECTRONICS, in IEEE Emerging and Selected Topics in Power Electronics and in IEEE Industrial Electronics Magazine.

Dr. Dragičević is a recipient of the Končar prize for the best industrial Ph.D. thesis in Croatia, and a Robert Mayer Energy Conservation award.